Remote Sensing of Environment xxx (2015) xxx–xxx

Contents lists available at ScienceDirect

Remote Sensing of Environment

journal homepage: www.elsevier.com/locate/rse

# Mesoscale assessment of changes in tropical tree species richness across a bioclimatic gradient in Panama using airborne imaging spectroscopy

Ben Somers [a,d,*], Gregory P. Asner [b], Roberta E. Martin [b], Christopher B. Anderson [b], David E. Knapp [b], S. Joseph Wright [c], Ruben Van De Kerchove [d]

[a] Division Forest, Nature & Landscape, KU Leuven, Celestijnenlaan 200E — bus 2411, B-3001 Leuven, Belgium
[b] Department of Global Ecology, Carnegie Institution for Science, 260 Panama Street, Stanford, CA 94305, USA
[c] Smithsonian Tropical Research Institute, Balbao, Ancon, Panama
[d] Flemish Institute for Technological Research (VITO), Centre for Remote Sensing and Earth Observation Processes (TAP), Boeretang 200, BE-2400 Mol, Belgium

ARTICLE INFO

*Article history:*
Received 15 June 2014
Received in revised form 2 April 2015
Accepted 8 April 2015
Available online xxxx

*Keywords:*
Biodiversity
Hyperspectral
Climate change
Spectral variation hypothesis
Alpha diversity
Beta diversity

ABSTRACT

We used imaging spectroscopy to perform a top-down mesoscale analysis of tropical tree species richness across a bioclimatic gradient in Panama. The expressed precipitation gradient from the wet Caribbean side to the dry Pacific side makes Panama an excellent study area for performing a mesoscale assessment of climate effects on tropical tree species richness. Spatial patterns in local spectral variability (expressed as the coefficient of variation) and spectral similarity (expressed as the spectral similarity index) were used as proxies for species area curves and species distance decay curves. Our analysis revealed significant spectral changes along the precipitation gradient. Highest spectral diversity was observed for moist forest sites while lowest diversity was observed for the driest forest sites. Most of the spectral variation came from changes in the visible (VIS) and shortwave-infrared (SWIR) reflectance. Variation in the VIS was significantly higher for the dry compared to the moist and wet forests, while the opposite was true for the NIR and SWIR reflectance. Our spectral mesoscale analysis extends previous results suggesting that niche differentiation with respect to soil water availability is a direct determinant of both local- and regional-scale distributions of tropical trees. A next step would be to test the accuracy and scalability of our results with lower spatial resolution spectrometer data, simulating the observing conditions that will be achieved with future satellite missions such as the European Union's EnMap and NASA's HyspIRI missions.



## 1. Introduction

Anticipated changes in regional and global climate could drive shifts in the geographic extent, composition and condition of tropical forest canopies (Collwell, Brehm, Cardelus, Gilman, & Longino, 2008; Wright, 2005). Biologists, conservationists and policy makers therefore raise concerns about alterations in the functioning of tropical forests and their capacity to sustain environmental services such as carbon storage and water provisioning (FAO, 2007; Foster, 2001). A need for thorough understanding of how the composition, structure and function of tropical forest canopies will respond to changing environmental conditions will increase as the rate of change accelerates (Schimel, Asner, & Moorcroft, 2013).

The evidence for a pantropical response to global anthropogenic forcing comes almost exclusively from relatively small-scaled censuses of tree plots (Wright, 2005). Although these networks of observations provide valuable insights to the fundamental processes governing canopy function, they lack scalability due to the extremely diverse nature of tropical canopies in terms of both floristic and structural variation, as well as their non-random or systematic placement across tropical land-cover types. An understanding of how tropical forests respond to environmental change requires scaling up our observation capability to the landscape level that captures entire forest communities and transitions between communities. Yet, our ability to measure, scale up and predict basic ecosystem function in tropical forests remains weak. This is strongly linked to practical and logistic difficulties in the often inaccessible tall forest canopies and the overwhelming local-scale (alpha) and regional-scale (beta, gamma) diversity of many tropical systems (Asner, 2013). The majority of work at the landscape scale has thus focused on general description of forest physiognomy, relatively small spatial domains, subsets of common species, or family-level taxonomy (e.g. Higgins et al., 2014).

Until recently, air- and spaceborne remote sensing was most useful for determining the spatial extent and dynamics of vegetation cover. However, technical developments in sensors and instrumentation have vastly improved the quantity and quality of information that can be obtained remotely, and advances in understanding how light interacts with plant canopies have made remote sensing increasingly useful for detecting patterns and analyzing processes related to the composition and functioning of vegetated ecosystems. Imaging spectroscopy, a

* Corresponding author.
*E-mail address:* ben.somers@ees.kuleuven.be (B. Somers).

http://dx.doi.org/10.1016/j.rse.2015.04.016
0034-4257/

remote sensing technology capable of measuring the earth's reflectance as a continuous spectrum of dozens to hundreds of narrow spectral bands across the visible and near-infrared spectral domain, has shown great potential to map the structure, function and composition of ecosystems at the "mesoscale" (e.g. Jusoff & Ibrahim, 2009; Ustin, Roberts, Gamon, Asner, & Green, 2004). The measured reflectance spectra are sensitive to the structural organization of, and variations in chemical constituents in, canopy components. These physico-chemical-to-spectral linkages provide a means of detecting species and/or functional types (e.g., Asner & Martin, 2009; Asner & Vitousek, 2005; Clark, Roberts, & Clark, 2005; Somers & Asner, 2012; Ustin & Gamon, 2010), and can even provide information about the biogeochemical heterogeneity (e.g. Townsend, Asner, & Cleveland, 2008; Vitousek, Asner, Chadwick, & Hotchkiss, 2009) and species richness of tropical forest canopies (e.g., Asner, Nepstad, Cardinot, & Ray, 2004; Carlson, Asner, Hughes, Ostertag, & Martin, 2007; Feret & Asner, 2013; Kalacska et al., 2007; Nagendra & Rocchini, 2008; Somers and Asner, 2013).

The remote mapping of biological and/or functional diversity is often done by analyzing variation of a particular spectral signal or spectral feature (Gould, 2000). This *Spectral Variation Hypothesis* (SVH) relies on the positive relationship between biological diversity and environmental heterogeneity, and has been used to map or detect biodiversity hotspots (alpha-diversity) and species turnover (beta-diversity) within and between a variety of ecosystems and communities (e.g., Gillespie, Foody, Rocchini, Giorgi, & Saatchi, 2008; Nagendra & Rocchini, 2008; Baldeck & Asner, 2013). Despite progress in the use of spectral variation to estimate biological diversity at different ecological scales, we still lack approaches needed to yield consistent and comparable biodiversity information across different ecosystems. This is particularly true in tropical regions where, for example, vegetation communities may vary from dry to humid forests often over short distances due to strong regional climate gradients (Condit, Ashton, Bunyavejchewin, et al., 2006). With global climate change, it is expected that the current environmental gradients under which forest assemblages formed may shift, and plant communities will be altered in response to those shifts. However, the extent, pattern, and rate of change in forest composition remain unknown, and most dynamic vegetation models lack the fine-scale geographic and biological resolution needed to predict plant community changes over time (Schimel et al., 2013).

New methods and technologies are critically needed to map and monitor changes in the functional and biological composition of ecosystems through time. Nowhere does this seem more critical than in tropical regions, such as Panama, where climate change and land use come together to place maximum pressure on forests and the ecological services they provide to society. Here we use airborne imaging spectroscopy to perform a top-down mesoscale analysis of changes in tropical tree species richness across a bioclimatic gradient in Panama. The expressed precipitation gradient from the wet Caribbean side to the dry Pacific side makes Panama an excellent study area. We sought to answer these specific questions: (i) Can we use airborne imaging spectroscopy to study spatial patterns in local (alpha) and regional (beta) tree species richness across tropical forests? (ii) Can we reveal significant changes in forest canopy spectral patterns, and thus canopy composition and diversity, along a precipitation gradient in Panama?; and if so (iii) are there specific spectral regions or wavelengths that dominate the spectral variation? In this study we seek to determine if imaging spectroscopy can be used to scale up previous results from plot-based studies providing a technology to track shifts in species richness due to climate change over broad spatial scales.

## 2. Material

### 2.1. Study area

The isthmus of Panama is dominated by a strong environmental gradient in climate, topography and geology. Average annual precipitation ranges from less than 1600 mm/yr on the Pacific side of the isthmus gradually increasing to over 3100 mm/yr on the Caribbean coast. At the highest elevations along the Caribbean coast precipitation can reach 4000 mm/yr (Rand & Rand, 1982). Rainfall is seasonal with a dry season from January through March, showing marked variation across sites, with an annual extreme moisture deficit around 500–600 mm at the driest sites but only between 300 and 400 mm in the wettest sides (Condit, Engelbrecht, Pino, Pérez, & Turner, 2013). The weathering pattern produced by the strong precipitation gradient has resulted in a complex geological terrain composed of either dense, relatively impermeable volcanic rock or porous, chemically unstable sedimentary rocks and volcanic mud flow deposits (Dietrich, Windsor, & Dunne, 1982).

Due to the variation in rainfall, Panama harbors a great diversity of tree species. The isthmus can broadly be divided into three general bioclimatic regions. On the wettest Caribbean slopes, there is enough moisture throughout the year to support evergreen tropical forests. In contrast, on the Pacific side many of the slopes have hard, dry soil by April. On this south-western side, many species are dry-season deciduous. In the middle of the country, lies moist tropical forest where the community transitions from dry to wet along the precipitation gradient. The trees increase in size and the occurrence of deciduousness lessens compared to dry forests, but does not disappear entirely (Condit, Pérez, & Daguerre, 2010). We selected a representative site of approximately 400 ha in each of the three bioclimatic regions (dry forest site: 7°26′50″N, 80°10′45″W; moist forest site: 9°4′32″N, 79°39′12″W; wet forest site: 9°16′50″N, 79°58′44″W) where both airborne imagery (see Section 2.3) and ground reference data (see Section 2.2) were available (Fig. 1).

### 2.2. Floristic data

For this study we used publicly available species lists collected from 18 permanent sampling forest plots (10 plots of 1 ha and 8 plots of 0.4 ha, Table 1) maintained by the Smithsonian Institution's Center for Tropical Forest Science (Condit, 1998; Pyke, Condit, Salamon, & Lao, 2001). For each plot all tree stems ≥ 10 cm DBH were identified and listed. These data were used to validate the spectral proxies for species richness and turnover (cf. Section 3.1.).

### 2.3. Remote sensing data and preprocessing

For each of the three study sites (Fig. 1) we used data collected from the Carnegie Airborne Observatory-2 Airborne Taxonomic Mapping Systems (CAO-2 AToMS; Asner et al., 2012). The imagery was acquired during January–February 2012 (i.e. the early dry season). AToMS includes a Visible-to-ShortWave InfraRed (VSWIR) imaging spectrometer and a dual laser, waveform LiDAR (Asner et al., 2012). These subsystems are boresight aligned onboard a Dornier 228-202 aircraft. Data were collected from an altitude of 2000 m above ground level, providing imagery with a 2 m spatial resolution, at an average flight speed of 55–60 m $s^{-1}$ and a mapping swath of 1.2 km.

The VSWIR spectrometer collects data in 480 contiguous spectral bands spanning the 252–2648 nm wavelength range with a spectral resolution of 5 nm. The VSWIR data were radiometrically corrected using a flat-field correction, radiometric calibration coefficients, and spectral calibration data collected in the laboratory. Apparent surface reflectance was derived from the radiance values using the ACORN-5 atmospheric correction model (Imspec LLC, Palmdale, CA). To improve aerosol corrections, ACORN-5 was run iteratively with different visibilities until the reflectance at 420 nm (i.e. almost constant for vegetation) was 1%. The reflectance data were further corrected for cross-track brightness gradients using a bidirectional reflectance distribution function model (Colgan, Baldeck, Féret, & Asner, 2012). Full details on the preprocessing of the VSWIR data can be found in Asner et al. (2014) and Colgan et al. (2012).

Please cite this article as: Somers, B., et al., Mesoscale assessment of changes in tropical tree species richness across a bioclimatic gradient in Panama using airborne imaging s..., *Remote Sensing of Environment* (2015), http://dx.doi.org/10.1016/j.rse.2015.04.016

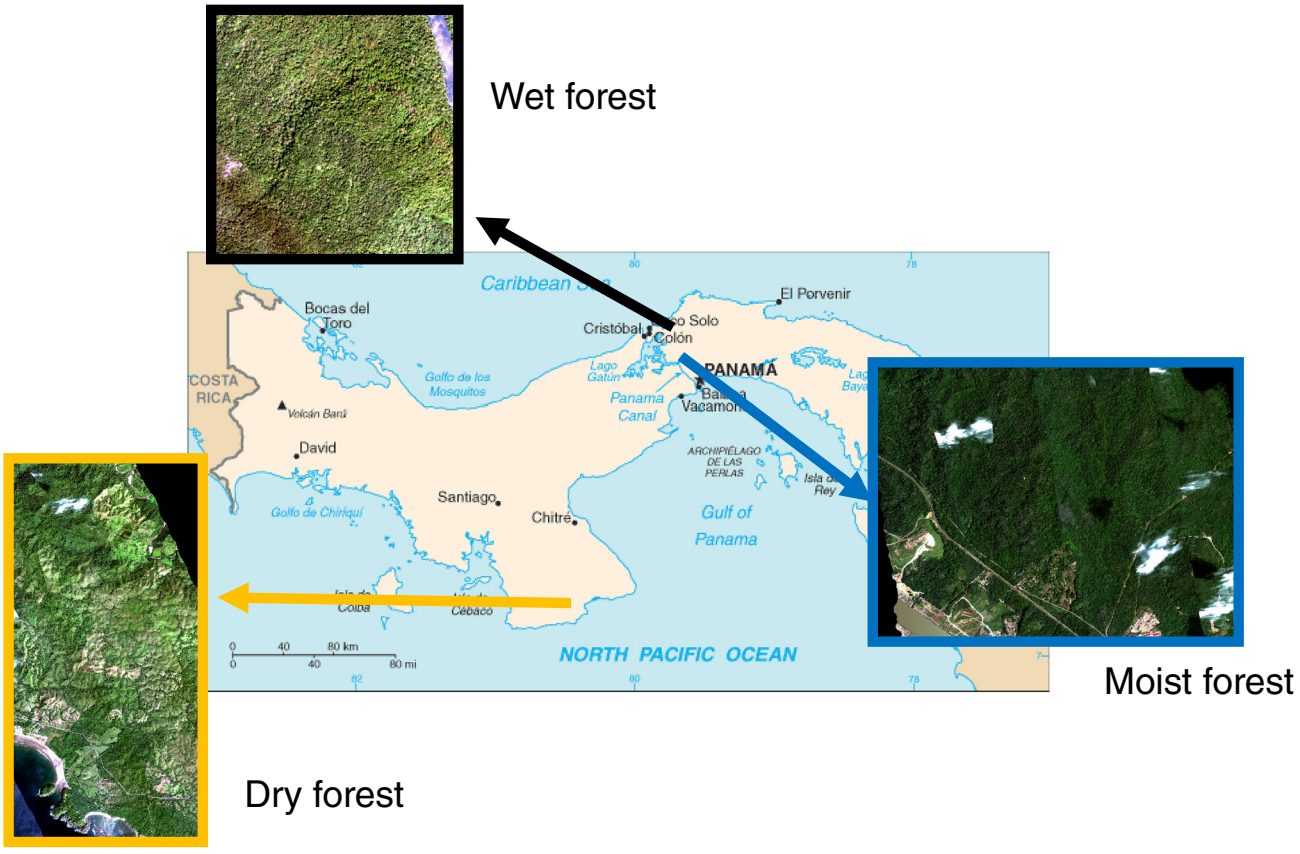


**Fig. 1.** Panamanian isthmus and locations of the three study sites.

The LiDAR in the CAO-2 AToMS is a dual-laser scanning system operating at 1064 nm. The LiDAR collects the full waveform with up to four discrete returns per laser shot. The LiDAR sub-system was configured such that the laser point density achieved was approximately 2 shots per square meter (or 8 shots per VSWIR pixel). From the LiDAR point cloud data, a physically-based model was used to estimate top-of-canopy and ground surfaces using Terrascan/Terramatch (Terasolid Ltd., Jyväskylä, Finland) software packages. Vegetation height was then estimated by differencing the top-of-canopy and ground surface digital elevation models following the common approach for these data (e.g. Lefsky et al., 1999). These structural data allowed for automated masking of forest gaps, intra- and inter-canopy shadows, and minimum vegetation height in the VSWIR images (Asner et al., 2008). A minimum LiDAR vegetation height requirement of 5 m was applied to remove exposed ground areas and non-tree vegetation. The LiDAR raster resolution was 1 m. In addition, a NDVI mask was applied (all pixels with a NDVI value < 0.4 were ignored) to exclude all remaining nonphotosynthetically active vegetation (NVP) and man-made materials (e.g. buildings). Subsequently, clouds and cloud shadows were manually masked. The remaining sunlit canopy spectra were used to analyze spatial patterns in forest canopy diversity and composition.

## 3. Methods

### 3.1. Validation of remotely sensed proxies of tree species richness

Research on plant species diversity and abundance mapping using remote sensing are broadly based on the Spectral Variation Hypothesis (SVH; e.g. Palmer, Earls, Hoagland, White, & Wohlgemuth, 2002; Rocchini, Balkenhol, Carter, et al., 2010) which relies on the assumption that spectral heterogeneity can be used to quantify (species) diversity. The obtained species diversity patterns are in turn believed to also be related to environmental (ecosystem) heterogeneity, based on the 'portfolio effect' (Rocchini et al., 2010). The SVH has been mainly used for two purposes: (1) the mapping or detection of biodiversity hotspots (so-called α-diversity); and (2) the development of quantitative measures for species turnover between ecosystems (so-called β-diversity).

Several recent studies have, indeed, verified that local spectral variability in remote sensing data correlates with local plant species richness (i.e. the number of species per unit area; e.g. Rocchini, 2007) in a variety of ecosystems. Many of these studies showed that measures of dispersion, such as the coefficient of variation (CV), are simple and effective indicators of spectral heterogeneity per sampling unit (e.g. an

**Table 1**
Basic summary information on number (and size) of plots per forest type and response variable (species richness).

| | 0.4 ha plots | | 1 ha plots | |
|---|---|---|---|---|
| | Number of plots | Average species richness (and standard deviation) | Number of plots | Average species richness (and standard deviation) |
| Dry forest site | 1 | 35 (NA) | 1 | 59 (NA) |
| Moist forest site | 7 | 78 (16) | 5 | 80 (11) |
| Wet forest site | 2 | 73 (5) | 2 | 80 (2) |

Please cite this article as: Somers, B., et al., Mesoscale assessment of changes in tropical tree species richness across a bioclimatic gradient in Panama using airborne imaging s..., *Remote Sensing of Environment* (2015), http://dx.doi.org/10.1016/j.rse.2015.04.016

image window/kernel) (e.g. Carter, Knapp, Anderson, Hoch, & Smith, 2005; Duro et al., 2014; Levin, Shmida, Levanoni, Tamari, & Kark, 2007; Lucas & Carter, 2008). Here we employed the CV (Eq. 1) to link the spectral heterogeneity within the 1 ha or 0.4 ha area of the field plots (equivalent to a sampling window of 50 by 50 (1 ha) and 32 by 32 (0.4 ha) image pixels respectively), to the field species counts within the field plots (cf. Section 2.2).

$$CV = \frac{1}{n}\sum_{b=0}^{n}\frac{sd(R_b)}{mean(R_b)} \quad (1)$$

With $R_b$ the reflectance in band $b$ and $n$ the total number of bands. CV can either be calculated for the full spectrum, a part of the spectrum or on a per waveband basis. In the latter case $n$ equals 1. CV increases with increasing spectral variability and is, according the SVH hypothesis, as such, a measure for species richness, a common measure of alpha-diversity (Rocchini, Dadalt, Delucchi, Neteler, & Palmer, 2014, Rocchini et al., 2013). Since CV is a bounded variable, regression analysis was performed using a General Linear Model with a Gamma error distribution.

The SVH further suggests that beta-diversity or species turnover can be quantified using the spectral distance (i.e. the spectral similarity) between different locations (or image pixel windows). The rationale is that, the more similar the spectral populations of two image pixel windows are, the more similar the species pools in both locations. In contrast, the larger the spectral distance between both populations, the more likely the species turnover is larger between the locations (Rocchini, Butini, & Chiarucci, 2005). Here we use the spectral similarity index (Eq. 2; Somers, Delalieux, Stuckens, Verstraeten, & Coppin, 2009, Somers, Delalieux, et al., 2010; Somers & Asner, 2012) to quantify the spectral overlap between two plots $i$ and $j$ across all study sites:

$$SI = \frac{1}{n}\sum_{b=0}^{n}\frac{(sd(R_{b,i}) + sd(R_{b,j})}{|\overline{R}_{b,i} - \overline{R}_{b,j}|}. \quad (2)$$

SI provides a straightforward way to calculate the spectral distance between two populations for the full spectrum, a part of the spectrum or on a per waveband basis (in this case $n$ equals 1). Smaller SI values were expected to correspond to smaller spectral similarity and thus higher beta-diversity (smaller species overlap).

Once calibrated, these spectral diversity measures permit a metascale assessment of the canopy composition and diversity in our study sites. We evaluated CV (Eq. 1) as an indicator for species richness at the local/site scale (high alpha-diversity), and used SI to provide information on differences among sites in terms of turnover in species composition (beta-diversity).

### 3.2. Mesoscale assessment of tree species richness along a bioclimatic gradient

#### 3.2.1. Local diversity patterns through species area curves

In order to evaluate the differences in local diversity patterns between the three bioclimatic regions, we created spectral proxies for the relationship between species richness and area by calculating CV (i.e. a proxy for alpha diversity) for different image kernel/window sizes. Species-area relationships (SARs) or species area curves (SACs), measure how the number of observed species increases with increasing sample area, and constitute one of the most important and robust tools to characterize patterns in local diversity (Gotelli & Colwell, 2001). Therefore the spectral proxies of the SACs are an essential tool to test our hypothesis that climate processes are responsible for patterns of local diversity. In addition, SACs facilitate comparisons of measurements at different spatial scales.

#### 3.2.2. Patterns in species turnover through distance decay curves

Species area curves give an idea of the rate of change in species richness but do not give insight in how and at which rate species composition changes among sites. An important approach to measure spatial variation in beta diversity or species turnover is the distance-decay of community similarity. Distance-decay studies regress pair-wise measures of sample-unit similarity against pair-wise spatial distance, and parameterize a 'slope' that indicates the relative change in compositional similarity through geographic space (Morlon et al., 2008). Through calculating the spectral similarity between plots (quantified as SI, Eq. 2) at different spatial distances we could generate a spectral proxy for the Distance-Decay curve. These spectral distance-decay curves allowed us to assess spatial patterns in species turnover or beta diversity.

For each of the three study sites the spectral species area and distance decay curves were calculated for each location (i.e. each image pixel). This is done using a moving window approach. For each pixel CV and SI were calculated for a series of image windows, which were square kernels of $3 \times 3$ to $45 \times 45$ pixels. This allowed reconstruction of the species area and distance decay curves for each individual image pixel. The spectral proxies were first averaged over the entire spectrum and also calculated for each waveband separately. The spectral proxies, calculated using individual bands or the whole spectrum, and relationships derived from them were combined to assess spatial patterns in species diversity along the bioclimatic gradient. Statistical analysis was performed using version 3.0.2 of the 64-bit version of R, a multi-platform, open-source language and software for statistical computing (R Development Core Team, 2010). All statistical analyses were evaluated against the 95% confidence interval.

## 4. Results

### 4.1. Validation of remotely sensed proxies of tree species richness

In line with previous reports (Carter et al., 2005; Lucas & Carter, 2008; Rocchini et al., 2013, 2014), the spectral variation, quantified as CV averaged over all bands, showed a significant ($p < 0.001$) positive correlation with species richness or alpha diversity in our study area (residual deviance = 1.01; Fig. 2).

Also corresponding to previous results, the spectral similarity between plots proved to be a reliable proxy for species turnover or beta diversity (Fig. 3). Using SI, we successfully modeled the pairwise

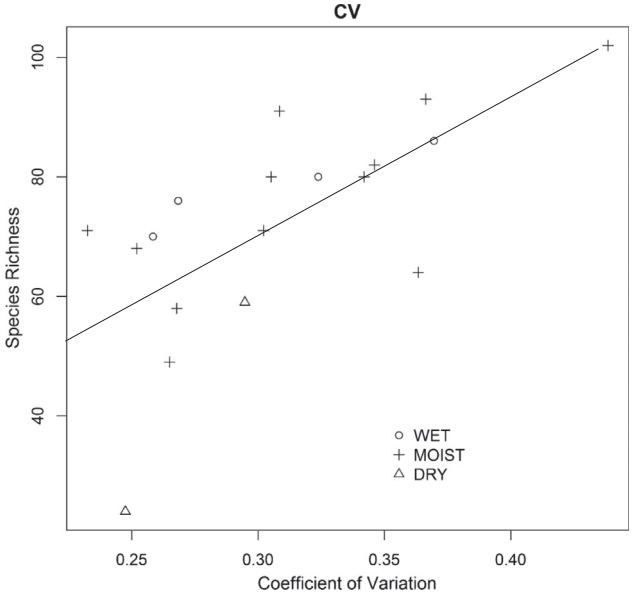


**Fig. 2.** Scatterplot showing the number of species observed in the 18 sampling forest plots (Section 2.2) against the coefficient of spectral variation averaged over all wavebands. A GLM model with a gamma error distribution showed a significant positive correlation between both variables (p-value < 0.001 and residual deviance = 1.01).

Please cite this article as: Somers, B., et al., Mesoscale assessment of changes in tropical tree species richness across a bioclimatic gradient in Panama using airborne imaging s..., *Remote Sensing of Environment* (2015), http://dx.doi.org/10.1016/j.rse.2015.04.016

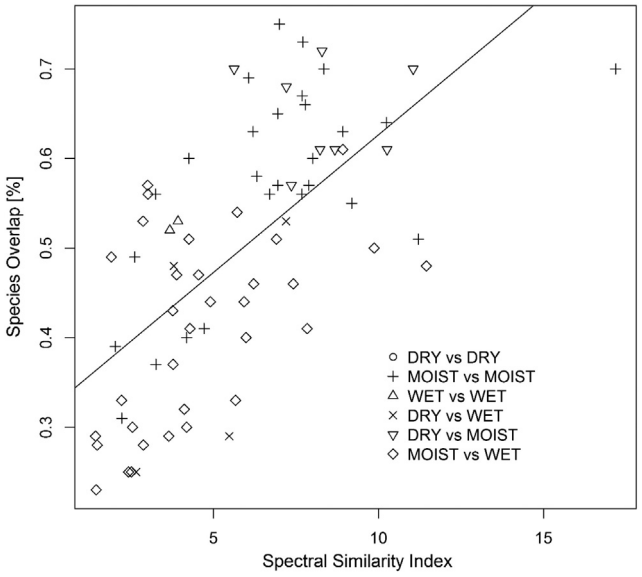


**Fig. 3.** Pairwise comparison of the spectral overlap between different plots (the SI index averaged over all wavebands) and the percentage of species that are common within the sampling forest plots.

comparisons of species overlap ($R^2 = 0.47$; $p < 0.001$). These results highlight the feasibility of using spectral proxies to perform a mesoscale assessment of changes in tree species richness along the bioclimatic gradient in our study area.

### 4.2. Mesoscale assessment of tree species richness along a climate gradient

#### 4.2.1. Local diversity patterns through species area curves

For each of the three sites, the average spectral variability–area curves (see 3.2. and Fig. 4), which can be considered variograms, reflect typical species-area relationships, with a near linear increase in spectral variability (species number) with area at smaller spatial scales which becomes shallower with increasing spatial extent until it finally plateaus (Scheiner, 2003). For all three sites maximal spectral variability (proxy for species richness), quantified as the CV averaged over the full spectrum, was reached at an image window size of 21 by 21 pixels (corresponding to a ground area of 42 by 42 m or approximately

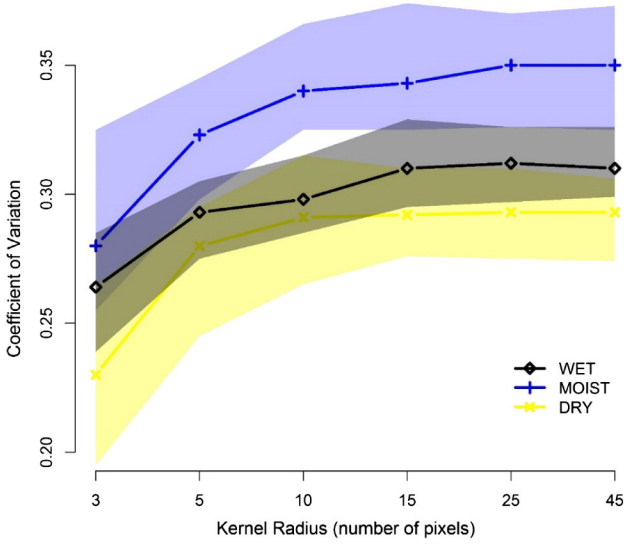


**Fig. 4.** Average CV as a function of kernel size (i.e. spectral proxy for species area curves) and 95% confidence interval for the three different study sites. Note that we used squared kernels.

0.18 ha). Yet, a Mann–Whitney–Wilcoxon Test revealed significant differences (p-value < 0.001) in the total area under the CV curve (Fig. 4) among the different sites. The test confirmed a distinctively higher spectral variability for the moist forest site at all spatial scales compared to both wet and dry forests (about 15% higher). Also, significantly higher spectral variation was observed for the wet compared to the dry forests, yet the main difference between both sites was the clearly smaller variation in the distribution of CV values for the wet site as displayed in the maps of Fig. 5 showing the spatial variation in the total area under the spectral species area curve. It is clear that most of the wet forest area is characterized by a stable spectral variability–area relationship (sum of CV for individual pixels averaged over all n bands ranges between 1 and 1.4, green/yellow) while only a limited area of low (sum of CV below 1, dark green) and high spectral diversity (sum of CV above 1.4, orange/red) are present. In the dry site we see similar patterns with more areas with a low index value (sum of CV below 1, dark green) and fewer areas with high index values (sum of CV above 1.6, red). The ecosystem with the highest alpha diversity was the moist forest with many large areas with index values exceeding 1.6 (Fig. 5, red).

Calculating the spectral variability–area curves on a per wavelength basis, as shown in Fig. 6, revealed subtle yet significant differences in spectral properties, and by correlation canopy chemical composition, among the different sites. For all three sites the spectral variability in the near-infrared (NIR, 700–1400 nm) was moderate (CV around 0.2) when compared to the visible (VIS, 350–700 nm) and shortwave-infrared (SWIR, 1400–2500 nm) (CV up to 0.45; Fig. 6). Most of the spectral variation in the VIS region was observed in the dry sites ($CV_{dry}$ up to 0.35 vs 0.33–0.34 for moist and wet sites respectively, Fig. 6). A Mann–Whitney–Wilcoxon test, indeed revealed significantly (p-value = 0.015) higher values for the total area under the CV curve in the VIS domain for the dry compared to the wet and moist sites. In contrast, moist and wet sites displayed significantly (p-value < 0.001) higher variability across the full spectrum and in the SWIR region (Fig. 6). The VIS (p-value = 0.009) and SWIR (p-value <0.001) reflectance of the dry sites was significantly higher than that of the two other sites (left panel of Fig. 7) reflecting lower levels of canopy water content (water absorbs SWIR reflectance) and canopy chlorophyll (pigments strongly absorb light in the visible spectrum) and/or more exposure of bark spectral properties (i.e. bark having high VIS and SWIR reflectance) during the dry season (Clark & Roberts, 2012).

#### 4.2.2. Patterns in species turnover through distance decay curves

To fully assess and understand the effects of climate on tropical tree species richness, we need information on species turnover as well. Recall from Section 4.1. that the spectral similarity between different plots (quantified as SI) showed a significant positive relation to species turnover. A general assessment of the spectral similarity, shown in Fig. 7, revealed relatively high spectral differences between dry and wet areas, moderate differences between dry and moist, and small differences between moist and wet areas. The small differences between moist and wet areas were apparent for the full spectrum (Fig. 7). However, the wet forest showed a slightly lower reflectance in the VIS compared to both other sites (Fig. 7). This can partly be assigned to more photosynthetically active radiation that is absorbed and thus foliar pigment concentrations that are higher. Differences in NIR reflectance between the dry site and the wet and moist sites were relatively small (SI > 15).

The patterns in species turnover (or spectral similarity index, SI), occurring among locations within each of the bioclimatic regions, indicate subtle differences as shown in Fig. 8. Slightly lower spectral similarity at all spatial scales was observed for the dry forest compared to the moist forest which in turn showed slightly less similarity compared to the wet forest. The precipitation signal is especially expressed in the VIS and NIR. The similarity in these spectral domains is clearly higher for the wet compared to the moist site (Fig. 9). In the dry sites we noticed that spectral differences were most pronounced at forest edges as illustrated in

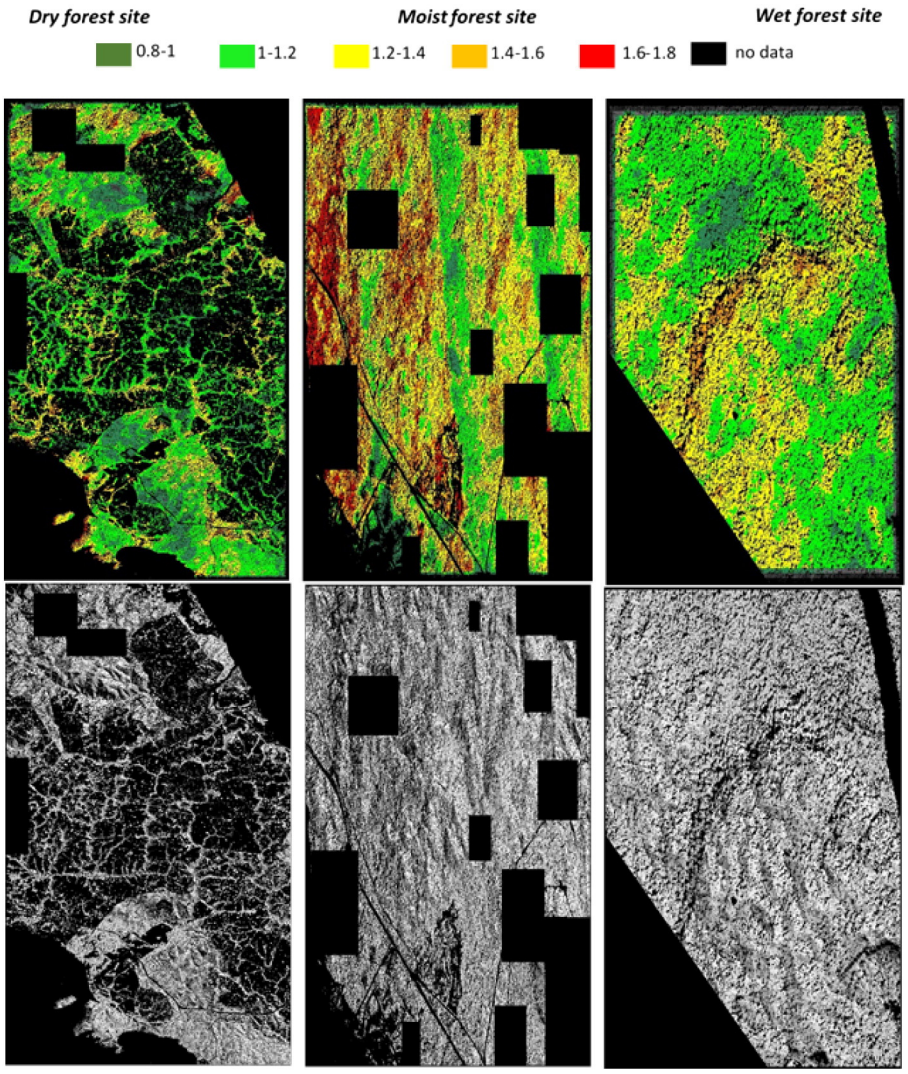


**Fig. 5.** (top) Map of the total area under the spectral proxy for SACs (i.e. change in CV with kernel size, Section 3.2) for the three study sites. CV is calculated here for individual pixels and averaged over all n bands. Dark green areas represent values of total area under the CV curve ranging between 0.8–1, light green between 1–1.2, yellow between 1.2–1.4, orange between 1.4–1.6, and red between 1.6–1.8. Black rectangles in the left and middle panel indicate cloud and cloud shadows that were manually masked from the analysis; (bottom) the corresponding hillshaded DEM derived from the LiDAR data. (For interpretation of the references to color in this figure legend, the reader is referred to the web version of this article.)

Fig. 10 showing a map of the total area under the spectral distance decay curve (Fig. 8).

## 5. Discussion and conclusions

We used airborne imaging spectroscopy as spectral proxies for local (alpha) and regional (beta) diversity, and revealed significant changes in spectral properties along a precipitation gradient in Panama. Spatial patterns in local spectral variability and spectral similarity were used as proxies for species area curves and species distance decay curves.

The spectral species area curves revealed a lower spectral diversity for the dry forest at all spatial scales as compared to the wet and moist forest sites (Figs. 4 and 5). This corroborates previous results of among others Gentry (1988) who showed that species richness increases with rainfall in Neotropical forests and reaches an asymptote at about 4 m annual rainfall. The number of species adapted to the severe seasonal dry conditions is limited, resulting in an overall lower species diversity (Engelbrecht et al., 2007; Gentry, 1988). More remarkable, however, we found distinctly higher spectral variability throughout the moist forest compared to the wet forest (Figs. 4 and 5). We found that, on average, the spectral variability (expressed as total area under the spectral proxy for SACs (i.e. change in CV with kernel size, Section 3.2.); Figs. 4 and 5) is significantly higher (about 15%) for the moist compared to the wet forest site. This tendency towards higher spectral variability in the moist site is also nicely illustrated in the maps of Fig. 5. Our results as such suggest an intermediate peak in tree species richness in the moist forest as compared to the dry or wet forests in our study area. This partly contradicts earlier reports of Pyke et al. (2001) who found a greater tree species richness on the wetter side of the Panamanian isthmus. Yet, in our subsample of the different forest types, the moist forest plots were slightly richer in species compared to the wet forest (i.e. average of 73 compared to 78 species/0.4 ha plot in wet compared to the moist plots respectively; in the 1 ha plots on average approximately 80 tree species were observed in both the moist and wet forest sites; here we need to note that only four samples were available for the wet forests so that these numbers are mainly indicative rather than providing significant proof of the differences between the sites, Table 1).

An additional explanation can be the increased occurrence of lianas in the moist forests. Schnitzer (2005) developed the hypothesis that lianas reach peak species richness at intermediate rainfall. Our results could as such suggest that trees plus canopy lianas reach peak species

Please cite this article as: Somers, B., et al., Mesoscale assessment of changes in tropical tree species richness across a bioclimatic gradient in Panama using airborne imaging s..., *Remote Sensing of Environment* (2015), http://dx.doi.org/10.1016/j.rse.2015.04.016

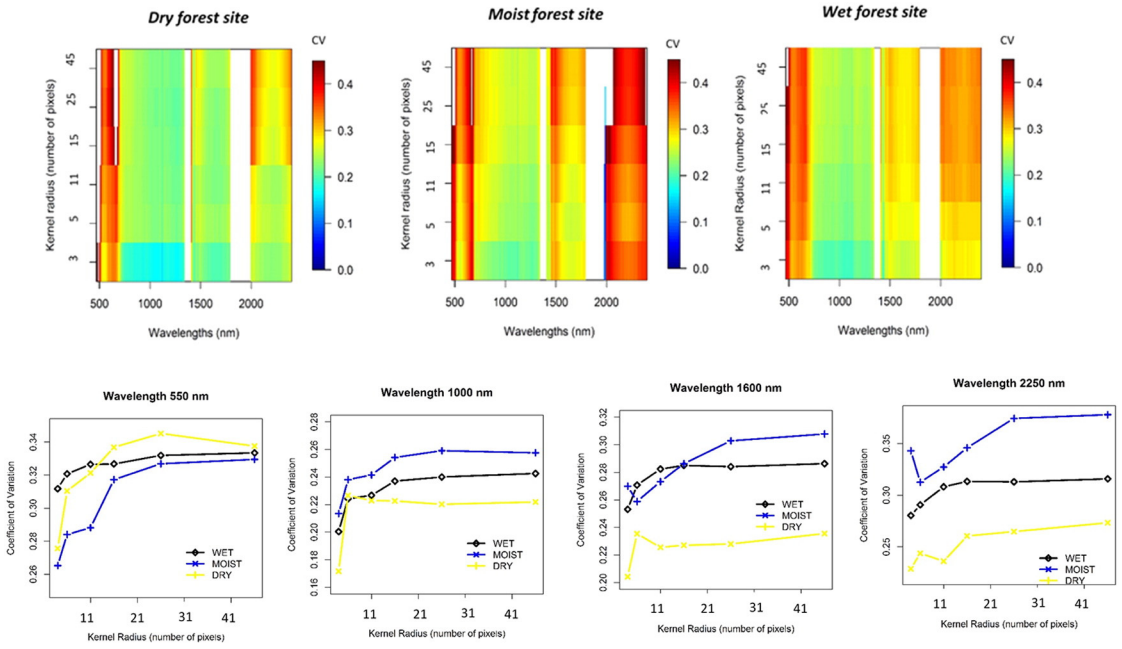


**Fig. 6.** Average spectral variability per wavelength (expressed as CV) for each site as a function of kernel size. Note that white areas represent off-the-scale, high CV values.

richness in the intermediate, moist forest. Increased epiphyte load and epiphylls on mature leaves might further add to the higher spectral diversity observed in the moist forest (Clark & Clark, 1990).

Another consideration is that the moist forests have greater variability in topography, which can be seen from the hill shaded DEMs in the bottom panels of Fig. 5. Topography affects cloud cover (insolation), precipitation, and temperature variability. This increased variation in environmental conditions, which may be more pronounced in the dry season when imagery were acquired, strongly drives (variation in) plant species composition (Pau et al., 2013). Comparison of the hill-shaded DEMs and the CV and SI index maps shown in Figs. 5 and 10, suggests a tendency towards higher CV and SI values around topographic transition zones for the moist forest site, a relationship which is less expressed in the wet forest site. This likely prominent topographic control on spectral diversity in the moist forests might further explain the observed higher spectral diversity in these sites.

A detailed analysis of the spectral variability on a per wavelength basis (Fig. 6) further indicated that most of the spectral variation comes from changes in the VIS and SWIR reflectance. Most interesting was the observation that the variation in the VIS was significantly higher for the dry compared to the moist and wet forests, while the opposite was true for the NIR and SWIR reflectance (Fig. 6). Broadly spoken we can state that leaf traits related to light capture and growth (for example, photosynthetic pigments, nutrients and leaf mass) are absorbing and scattering light roughly in the 350–700 nm spectral range (e.g., Asner, 1998; Ollinger, 2011). Secondary metabolites such as lignin, cellulose, phenols, and tannins, which contribute to foliar defense and longevity are active absorbers and scatterers of the NIR and SWIR electromagnetic energy (e.g., Kokaly, Asner, Ollinger, Martin, & Wessman, 2009; Majeke, van Aardt, & Cho, 2008). This latter spectral region is also strongly sensitive to water absorption (e.g., Ceccato, Flasse, Tarantola, Jacquemoud, & Gregoire, 2001).

The observed high variation of VIS reflectance in the dry forests might as such reflect a strategy to maximize photosynthesis when water is available and to minimize water loss and respiration costs during rainless periods (Brodribb, Holbrook, Edwards, & Gutierrez, 2003). Dry forest canopies are indeed characterized by an increasing leaf thickness, decreasing specific leaf area (SLA), shorter leaf life spans, relatively high P values and more enriched foliar N values suggesting greater resorption and re-metabolism of leaf N in drier forests (Santiago, Kitajima, & Wright, 2004). Oppositely, it has been reported that spatial variation in canopy composition in wet forests is strongly driven by

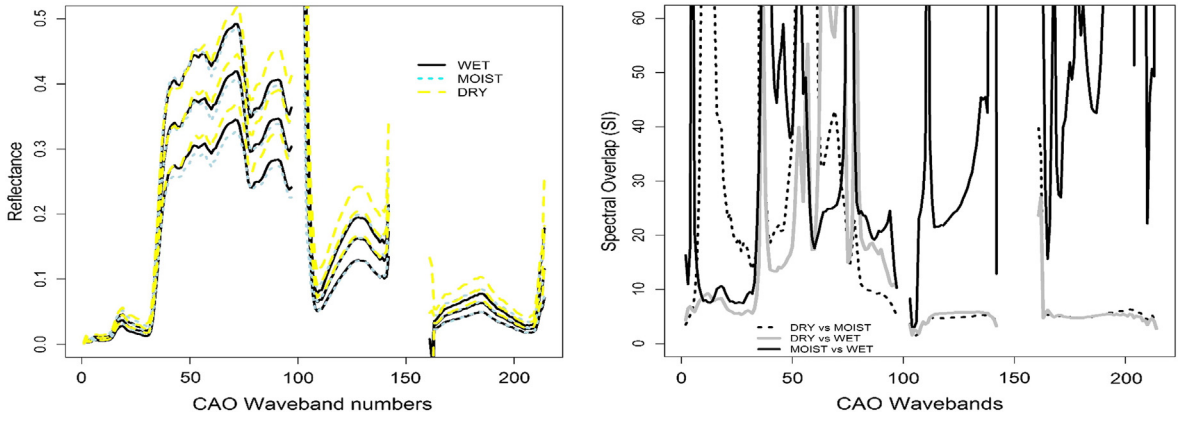


**Fig. 7.** (Left) Mean and standard deviation of the reflectance of all pixels within each of the three sites; (right) pairwise comparison of the spectral similarity (quantified as SI, Eq. 2) between sites.

Please cite this article as: Somers, B., et al., Mesoscale assessment of changes in tropical tree species richness across a bioclimatic gradient in Panama using airborne imaging s..., *Remote Sensing of Environment* (2015), http://dx.doi.org/10.1016/j.rse.2015.04.016

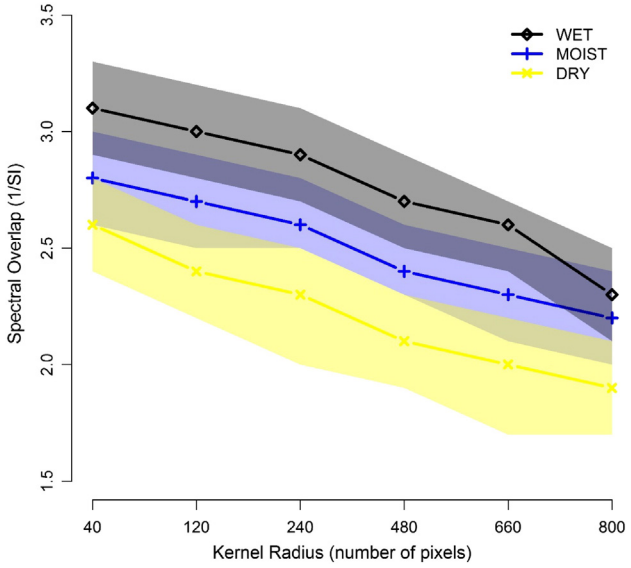


**Fig. 8.** Average decrease in spectral similarity (SI) with kernel size (i.e. spectral proxy for species distance decay curves) and 95% confidence interval for the three different study sites.

pathogens and pests and the higher variation in SWIR reflectance associated to a variation in leaf traits related to foliar defense and longevity is as such not surprising (Asner et al., 2011). Indeed, wet forest canopies are typically characterized by extended leaf longevity, more structural defense, higher midday leaf water potential and lower $P_{mass}$, $N_{mass}$ and SLA (Santiago et al., 2004). These differences in leaf traits for the dry compared to the wet and moist site are further highlighted when studying the spectral similarity (or species turnover) between the different forest sites (Fig. 7). Results in Fig. 7 clearly show higher absolute VIS and SWIR reflectance values (not variability but absolute reflectance values) for the dry sites.

Along our ecological gradient we also observed an impact on the spatial patterns in spectral similarity (i.e. beta diversity; Fig. 9). We observed a higher spectral similarity, especially in the VIS and NIR, throughout the wet compared to the moist and dry forests. The higher spectral variation in dry forests could predominantly be linked to habitat fragmentation resulting in increased availability of light resulting in more pronounced canopy pigmentation and a blend of interior, successional and invasive species near forest edges (Raghubanshi & Tripathi, 2009; Fig. 10). Also the clear contrast in water content and leaf conditions from riparian drainage to surrounding areas is likely contributing to the increased spectral variation (Laurance, Ferreira, Rankin-de Merona, & Laurance, 1998).

Yet, our interpretation explaining spectral variability based on differences in leaf traits and tree species richness requires additional considerations on other factors driving spectral variation among the different forest sites. For example, the relatively high spectral variation in VIS reflectance observed in the dry forests might to some extent also be influenced by the observation window. Since the airborne data were collected during the early dry season many dry forest drought deciduous trees occur in leaf-off conditions exposing more bark, epiphytes and dry background to the sensor; components all showing relatively high VIS reflectance (Clark & Roberts, 2012; Somers, Verbesselt, et al., 2010; Toomey, Roberts, & Nelson, 2009). In addition, many dry forest tree species flower in the dry season (Wright & Van Schaik, 1994) again adding to the VIS reflectance variability (flowers have high VIS reflectance; Clark et al., 2005). Another remarkable observation was that differences in NIR reflectance between the dry site and the wet and moist sites were relatively small (SI > 15), which could indicate that on average canopy structure and LAI were comparable. Yet, LiDAR derived histograms of the top-of-canopy (TCH) height (Fig. 11) indeed verified the similar canopy structure between wet (mean TCH = 23.67 m; sd = 7.77 m) and moist sites (mean TCH = 22.13 m; sd = 7.45 m) but revealed a distinctly lower TCH for the dry site (mean TCH = 10.73 m, sd = 6.37 m). Perhaps high NIR from dry herbaceous/soil background and bark exposed in the IFOV elevate NIR in dry forests to similar levels of moist and wet forests, which in those forests are more likely due to volumetric scattering among leaves. To conclude, differences in leaf and reproductive phenology, canopy structure, and contribution of other components (e.g. epiphylls, bark, background) are as such additional sources of spectral variation among forest sites that contribute to the within-species variability (and spectral variation; Zhang, Rivard, Sanchez-Azofeifa, & Castro-Essau, 2006) thereby attenuating the direct link with tree species richness.

This taken into account we can still state that our spectral mesoscale analysis extends previous results suggesting that niche differentiation with respect to soil water availability is a direct determinant of both local- and regional-scale distributions of tropical trees (Condit et al., 2013). Changes in soil moisture availability caused by global climate change and forest fragmentation are therefore likely to alter tropical species distributions, community composition and diversity (Engelbrecht et al., 2007; Pyke et al., 2001). We thus contend that the Panamanian forest shows clear patterns of spatial organization along environmental gradients, predominantly determined by broad-scale precipitation variation, but also partly driven by within-site variation related to topography and controls on fine-scale abiotic gradients.

Our results indicate that relative differences in tropical forest canopy diversity may be monitored using high-resolution imaging spectroscopy. A next step would be to test the accuracy and scalability of our results with lower spatial resolution spectrometer data, simulating the observing conditions that will be achieved with future satellite missions

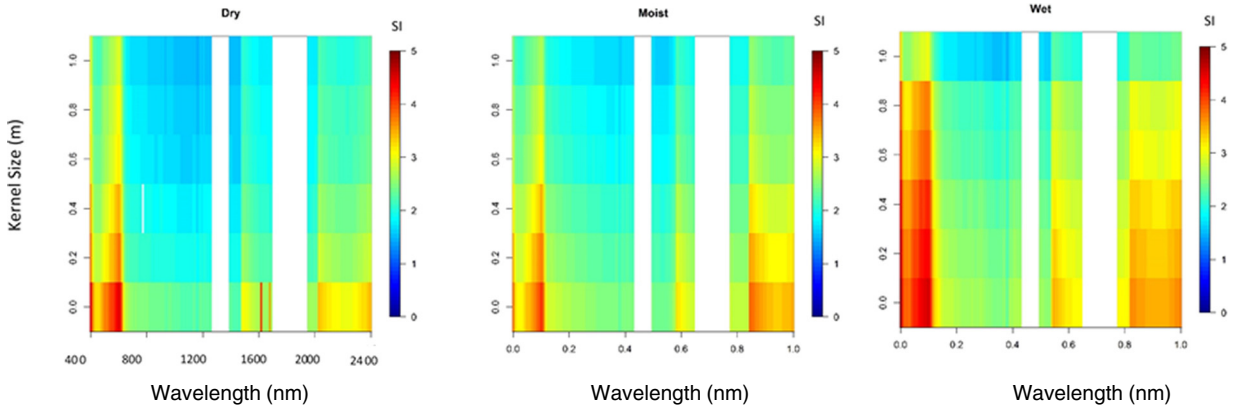


**Fig. 9.** Spectral overlap per wavelength (expressed as SI) as a function of kernel size.

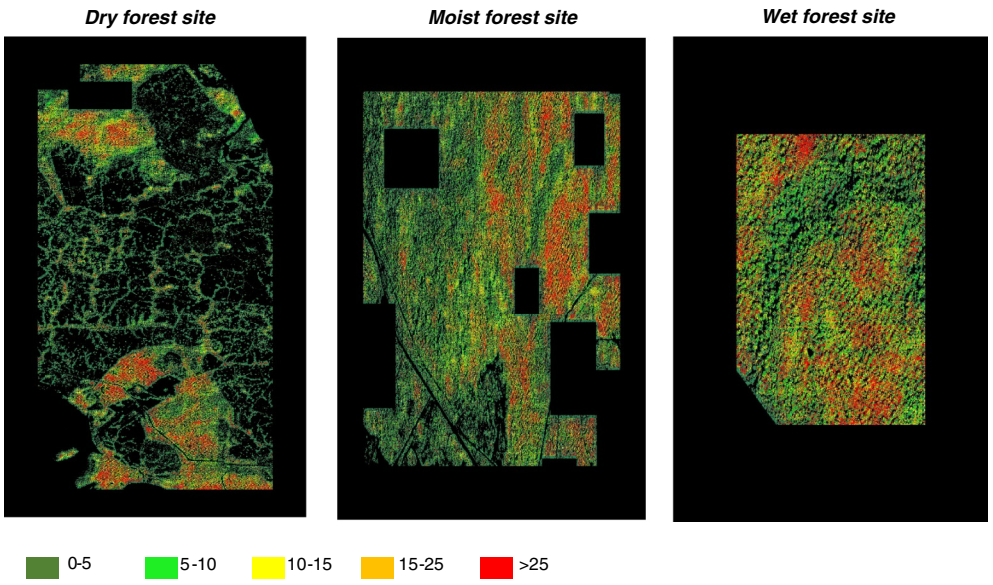


**Fig. 10.** Map of the total area under the spectral distance decay curve (Fig. 8) for the three study sites. Higher values indicate that spectral similarity is higher and thus, by way of the positive correlation found in this study, species richness is lower.

such as the European Union's EnMap (Sang et al., 2008) and NASA's HyspIRI missions. These satellites will observe the land surface at spatial resolutions of 30–60 m, thereby incorporating multiple tropical forest canopies into individual measurement pixels. Future research will therefore focus on performing a comprehensive sensitivity analysis of spectral diversity measures with respect to spectral mixing and spatial scaling. These analysis can be performed based on synthetic EnMAP-, and HyspIRI-like imagery using Carnegie Airborne Observatory as input of an end-to-end simulation tool like EeteS (Segl et al., 2012). These synthetic representations at different spatial (and/or spectral scales) allow for pronouncing the highly amplified mixed pixel scenario typical for coarser resolution spaceborne remote sensing imagery from tropical areas. Transferring our findings from sub-canopy resolution spectroscopy from the Carnegie Airborne Observatory to these satellite missions will require not only developments in remote sensing methods but also in the way we understand and treat the organisms (trees, lianas, etc) that comprise the spectroscopic signal at multiple spatial scales.

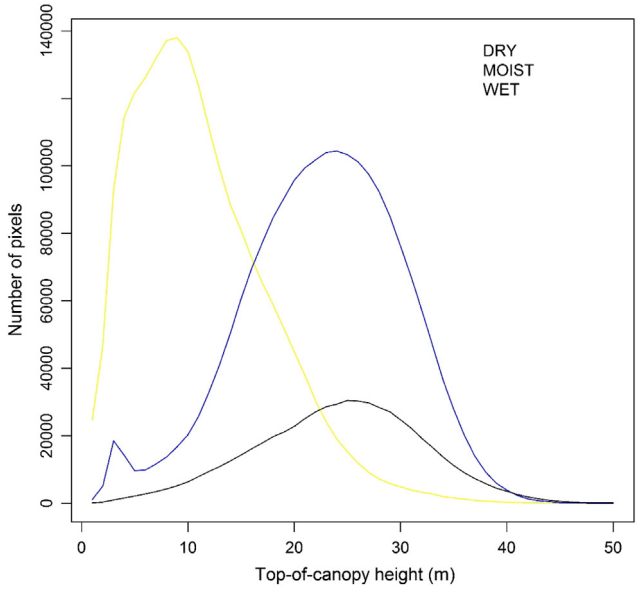


**Fig. 11.** Top-of-canopy height histograms derived from the LiDAR point clouds.

## Acknowledgments

The research presented in this paper is funded by the Belgian Science Policy Office in the framework of the STEREO II Program — Project ReMEDy (SR/67/164). The Carnegie Airborne Observatory is made possible by the Gordon and Betty Moore Foundation, the John D. and Catherine T. MacArthur Foundation, W. M. Keck Foundation, the Margaret A. Cargill Foundation, Grantham Foundation for the Protection of the Environment, Avatar Alliance Foundation, Mary Anne Nyburg Baker and G. Leonard Baker Jr., and William R. Hearst III. The plot project is part of the Center for Tropical Forest Science, a global network of large-scale demographic tree plots. This research is further supported by VLIR-UOS (Flemish Interuniversity Council — University Development Cooperation) and DGD (the Directorate General for Development Cooperation) (NOPO2014Pr0001) through the KLIMOS consortium.

## References

Asner, G. P. (1998). Biophysical and biochemical sources of variability in canopy reflectance. *Remote Sensing of Environment*, *64*, 234–253.

Asner, G. P. (2013). Mesoscale exploration and conservation of tropical canopies in a changing climate. In M. Lowman (Eds.), *Treetops at risk: Challenges of global canopy ecology and conservation*. Springer Science + Business Media New York.

Asner, G. P., Anderson, C. B., Martin, R. E., Knapp, D. E., Tupayachi, R., Sinca, F., et al. (2014). Landscape-scale changes in forest structure and functional traits along an Andes-to-Amazon elevation gradient. *Biogeosciences*, *11*, 843–856.

Asner, G. P., Knapp, D. E., Boardman, J., Green, R. O., Kennedy-Bowdoin, T., Eastwood, M., et al. (2012). Carnegie Airborne Observatory-2: Increasing science data dimensionality via high-fidelity multi-sensor fusion. *Remote Sensing of Environment*, *124*, 454–465.

Asner, G. P., Knapp, D. E., Kennedy-Bowdoin, T., Jones, M. O., Martin, R. E., Boardman, J., et al. (2008). Invasive species detection in Hawaiian rainforests using airborne imaging spectroscopy and LiDAR. *Remote Sensing of Environment*, *112*, 1948–1955.

Asner, G. P., & Martin, R. E. (2009). Airborne spectranomics: Mapping canopy chemical and taxonomic diversity in tropical forests. *Frontiers in Ecology and the Environment*, *7*, 269–276.

Asner, G. P., Martin, R. E., Knapp, D. E., Tupayachi, R., Anderson, C., Carranza, L., et al. (2011). Spectroscopy of canopy chemicals in humid tropical forests. *Remote Sensing of Environment*, *115*, 3587–3598.

Asner, G. P., Nepstad, D., Cardinot, G., & Ray, D. (2004). Drought stress and carbon uptake in an Amazon forest measured with spaceborne imaging spectroscopy. *Proceedings of the National Academy of Sciences of the United States of America*, *101*, 6039–6044.

Asner, G. P., & Vitousek, P. M. (2005). Remote analysis of biological invasion and biogeochemical change. *Proceedings of the National Academy of Sciences of the United States of America*, *102*, 483–486.

Baldeck, C. A., & Asner, G. P. (2013). Estimating vegetation beta diversity from airborne imaging spectroscopy and unsupervised clustering. *Remote Sensing*, *5*(5), 2057–2071.

Brodribb, T. J., Holbrook, N. M., Edwards, E. J., & Gutierrez, M. V. (2003). Relations between stomatal closure, leaf turgor and xylem vulnerability in eight tropical dry forest trees. *Plant, Cell & Environment*, *26*, 443–450.

Carlson, K. M., Asner, G. P., Hughes, R. F., Ostertag, R., & Martin, R. E. (2007). Hyperspectral remote sensing of canopy biodiversity in Hawaiian lowland rainforests. *Ecosystems, 10*, 536–549.

Carter, G. A., Knapp, A. K., Anderson, J. E., Hoch, G. A., & Smith, M. D. (2005). Indicators of plant species richness in AVIRIS spectra of a mesic grassland. *Remote Sensing of Environment, 98*, 304–316.

Ceccato, P., Flasse, S., Tarantola, S., Jacquemoud, S., & Gregoire, J. M. (2001). Detecting vegetation leaf water content using reflectance in the optical domain. *Remote Sensing of Environment, 77*, 22–33.

Clark, D. B., & Clark, D. A. (1990). Distribution and effects on tree growth of lianas and woody hemiepiphytes in a Costa Rican tropical wet forest. *Journal of Tropical Ecology, 6*, 321–331.

Clark, M. L., & Roberts, D. A. (2012). Species-level differences in hyperspectral metrics among tropical rainforest trees as determined by a tree-based classifier. *Remote Sensing, 4*, 1820–1855.

Clark, M. L., Roberts, D. A., & Clark, D. B. (2005). Hyperspectral discrimination of tropical rain forest tree species at leaf to crown scales. *Remote Sensing of Environment, 96*, 375–398.

Colgan, M., Baldeck, C., Féret, J. B., & Asner, G. P. (2012). Mapping savanna tee species at ecosystem scales using support vector machine classification and BRDF correction on airborne hyperspectral and lidar data. *Remote Sensing, 4*, 3462–3480.

Collwell, R. K., Brehm, G., Cardelus, C. L., Gilman, A. C., & Longino, J. T. (2008). Global warming, elevational range shifts, and lowland biotic attrition in the wet tropics. *Science, 332*, 258–261.

Condit, R. (1998). *Tropical forest census plots.* Berlin, Germany, and Georgetown, Texas: Springer-Verlag and R. G. Landes Company.

Condit, R., Ashton, P., Bunyavejchewin, S., Dattaraja, H. S., Davies, S., Esufali, S., et al. (2006). The importance of demographic niches to tree diversity. *Science, 313*, 98–101.

Condit, R., Engelbrecht, B. M. J., Pino, D., Pérez, R., & Turner, B. L. (2013). Species distributions in response to individual soil nutrients and seasonal drought across a community of tropical trees. *Proceedings of the National Academy of Sciences, 110*, 5064–5068.

Condit, R., Pérez, R., & Daguerre, N. (2010). *Trees of Panama and Costa Rica.* Princeton University Press.

Dietrich, W., Windsor, D., & Dunne, T. (1982). Geology, climate, and hydrology of Barro Colorado Island. In LeighJr. (Eds.), *The ecology of a tropical forest*. Washington, DC: Smithsonian Institution Press.

Duro, D. C., Girard, J., King, D. J., Fahrig, L., Mitchell, S., Lindsay, K., et al. (2014). Predicting species diversity in agricultural environments using Landsat TM imagery. *Remote Sensing of Environment, 144*, 214–225.

Engelbrecht, B. M. J., Comita, L. S., Condit, R., Kursar, T. A., Tyree, M. T., Turner, B. L., et al. (2007). Drought sensitivity shapes species distribution patterns in tropical forests. *Nature, 447*, 80–83.

FAO (2007). *State of the world's forests.* Rome: FAO.

Feret, J. -B., & Asner, G. P. (2013). Tree species discrimination in tropical forests using airborne imaging spectroscopy. *IEEE Transactions on Geoscience and Remote Sensing, 51*, 73–84.

Foster, P. (2001). The potential negative impacts of global climate change on tropical montane cloud forests. *Earth-Science Reviews, 55*, 73–106.

Gentry, A. H. (1988). Changes in plant community diversity and floristic composition on environmental and geographical gradients. *Annals of the Missouri Botanical Garden, 75*, 1–34.

Gillespie, T. W., Foody, G. M., Rocchini, D., Giorgi, A. P., & Saatchi, S. (2008). Measuring and modelling biodiversity from space. *Progress in Physical Geography, 32*, 209–221.

Gotelli, N. J., & Colwell, R. K. (2001). Quantifying biodiversity: Procedures and pitfalls in the measurement and comparison of species richness. *Ecology Letters, 4*, 379–391.

Gould, W. (2000). Remote sensing of vegetation, plant species richness, and regional biodiversity hotspots. *Ecological Applications, 10*, 1861–1870.

Higgins, M. A., Asner, G. P., Martin, R. E., Knapp, D. E., Anderson, C., Kennedy-Bowdoin, T., et al. (2014). Linking imaging spectroscopy and LiDAR with floristic composition and forest structure in Panama. *Remote Sensing of Environment*http://dx.doi.org/10.1016/j.rse.2013.09.032.

Jusoff, K., & Ibrahim, K. (2009). Hyperspectral remote sensing for tropical rainforest. *American Journal of Applied Sciences, 6*, 2001–2005.

Kalacska, M., Sanchez-Azofeifa, G. A., Rivard, B., Caelli, T., White, H. P., & Calvo-Alvarado, J. C. (2007). Ecological fingerprinting of ecosystem succession: Estimating secondary tropical dry forest structure and diversity using imaging spectroscopy. *Remote Sensing of Environment, 108*, 82–96.

Kokaly, R. F., Asner, G. P., Ollinger, S. V., Martin, M. E., & Wessman, C. A. (2009). Characterizing canopy biochemistry from imaging spectroscopy and its application to ecosystem studies. *Remote Sensing of Environment, 113*, S78–S91.

Laurance, W. F., Ferreira, L. V., Rankin-de Merona, J. M., & Laurance, S. G. (1998). Rain forest fragmentation and the dynamics of Amazonian tree communities. *Ecology, 79*, 2032–2040.

Lefsky, M. A., Cohen, W. B., Acker, S. A., Parker, G. G., Spies, T. A., & Harding, D. (1999). Lidar remote sensing of the canopy structure and biophysical properties of Douglas-fir western hemlock forests. *Remote Sensing of Environment, 70*, 339–361.

Levin, N., Shmida, A., Levanoni, O., Tamari, H., & Kark, S. (2007). Predicting mountain plant richness and rarity from space using satellite-derived vegetation indices. *Diversity and Distributions, 13*, 692–703.

Lucas, K., & Carter, G. (2008). The use of hyperspectral remote sensing to assess vascular plant species richness on Horn Island, Mississippi. *Remote Sensing of Environment, 112*, 3908–3915.

Majeke, B., van Aardt, J. A. N., & Cho, M. A. (2008). Imaging spectroscopy of foliar biochemistry in forestry environments. *Southern Forests, 70*, 275–285.

Morlon, H., Chuyong, G., Condit, R., Hubbell, S., Kenfack, D., Thomas, D., et al. (2008). A general framework for the distance-decay of similarity in ecological communities. *Ecology Letters, 11*, 904–917.

Nagendra, H., & Rocchini, D. (2008). High resolution satellite imagery for tropical biodiversity studies: The devil is in the detail. *Biodiversity and Conservation, 17*, 3431–3442.

Ollinger, S. V. (2011). Sources of variability in canopy reflectance and the convergent properties of plants. *New Phytologist, 189*, 375–394.

Palmer, M. W., Earls, P. G., Hoagland, B. W., White, P. S., & Wohlgemuth, T. (2002). Quantitative tools for perfecting species lists. *Environmetrics, 13*, 121–137.

Pau, S., Wolkovich, E. M., Cook, B. I., Nytch, C. J., Regetz, J., Zimmerman, J. K., et al. (2013). *Nature Climate Change, 3*, 838–842.

Pyke, C. R., Condit, R., Salamon, A., & Lao, S. (2001). Floristic composition across a climate gradient in a neotropical lowland forest. *Journal of Vegetation Science, 12*, 553–566.

R Development Core Team (2010). R: A language and environment for statistical computing. Available online: http://www.lsw.uni-heidelberg.de/users/christlieb/teaching/UKStaSS10/R-refman.pdf

Raghubanshi, A. S., & Tripathi, A. (2009). Effect of disturbance, habitat fragmentation and alien invasive plants on floral diversity in dry tropical forests of Vindhyan highland: A review. *Tropical Ecology, 50*, 57–69.

Rand, A., & Rand, W. (1982). Variation in rainfall on Barro Colorado Island. In LeighJr. (Eds.), *The ecology of a tropical forest*. Washington, DC: Smithsonian Institution Press.

Rocchini, D. (2007). Effects of spatial and spectral resolution in estimating ecosystem alpha-diversity by satellite imagery. *Remote Sensing of Environment, 111*, 423–434.

Rocchini, D., Balkenhol, N., Carter, G. A., Foody, G. M., Gillespie, T. W., He, K., et al. (2010). Remotely sensed spectral heterogeneity as a proxy of species diversity: Recent advances and open challenges. *Ecological Informatics, 5*, 318–329.

Rocchini, D., Butini, S. A., & Chiarucci, A. (2005). Maximizing plant species inventory efficiency by means of remotely sensed spectral distances. *Global Ecology and Biogeography, 14*, 431–437.

Rocchini, D., Dadalt, L., Delucchi, L., Neteler, M., & Palmer, M. W. (2014). Disentangling the role of remotely sensed spectral heterogeneity as a proxy for North American plant species richness. *Community Ecology, 15*(1), 37–43.

Rocchini, D., Delucchi, L., Bacaro, G., Cavallini, P., Feilhauer, H., Foody, G. M., et al. (2013). Calculating landscape diversity with information-theory based indices: A GRASS GIS solution. *Ecological Informatics, 17*, 82–93.

Sang, B., Schubert, J., Kaiser, S., Mogulsky, V., Neumann, C., Förster, K. -P., et al. (2008). *SPIE Proceedings, 7086*.

Santiago, L. S., Kitajima, K., & Wright, S. J. (2004). Coordinated changes in photosynthesis, water relations and leaf nutritional traits of canopy trees along a precipitation gradient in lowland tropical forest. *Ecophysiology, 139*, 495–502.

Scheiner, S. M. (2003). Six types of species-area curves. *Global Ecology and Biogeography, 12*, 441–447.

Schimel, D. S., Asner, G. P., & Moorcroft, P. R. (2013). Observing changing ecological diversity in the Anthropocene. *Frontiers in Ecology and the Environment, 11*, 129–137.

Schnitzer, S. A. (2005). A mechanistic explanation for the global patterns of liana abundance and distribution. *The American Naturalist, 166*, 262–276.

Segl, K., Guanter, L., Rogass, C., Kuester, T., Roessner, S., Kaufmann, H., et al. (2012). EeteS — the EnMAP end-to-end simulation tool. *IEEE Journal of Selected Topics in Applied Earth Observations and Remote Sensing, 5*, 522–530.

Somers, B., & Asner, G. P. (2012). Hyperspectral time series analysis of native and invasive species in Hawaiian rainforests. *Remote Sensing, 4*, 2510–2529.

Somers, B., & Asner, G. P. (2013). Multi-temporal mixture analysis and feature selection for invasive species mapping in rainforests. *Remote Sensing of Environment, 136*, 14–27.

Somers, B., Delalieux, S., Stuckens, J., Verstraeten, W. W., & Coppin, P. (2009). A weighted linear spectral mixture analysis approach to address endmember variability in agricultural production systems. *International Journal of Remote Sensing, 30*, 139–147.

Somers, B., Delalieux, S., Verstraeten, W. W., van Aardt, J. A. N., Albrigo, G. L., & Coppin, P. (2010a). An automated wavelength selection technique for optimized hyperspectral mixture analysis. *International Journal of Remote Sensing, 31*, 5549–5568.

Somers, B., Verbesselt, J., Ampe, E. M., Sims, N., Verstraeten, W. W., & Coppin, P. (2010b). Spectral mixture analysis to monitor defoliation in mixed aged Eucalyptus globules Labill plantations in southern Australia using Landsat 5TM and EO-1 Hyperion data. *International Journal of Applied Earth Observation and Geoinformation, 12*, 270–277.

Toomey, M., Roberts, D. A., & Nelson, B. (2009). The influence of epiphylls on remote sensing of humid forests. *Remote Sensing of Environment, 113*, 1787–1798.

Townsend, A. R., Asner, G. P., & Cleveland, C. C. (2008). The biogeochemical heterogeneity of tropical forests. *Trends in Ecology & Evolution, 23*, 424–431.

Ustin, S. L., & Gamon, J. A. (2010). Remote sensing of plant functional types. *New Phytologist, 186*, 795–816.

Ustin, S. L., Roberts, D. A., Gamon, J. A., Asner, G. P., & Green, R. O. (2004). Using imaging spectroscopy to study ecosystem processes and properties. *BioScience, 54*, 523–534.

Vitousek, P., Asner, G. P., Chadwick, O. A., & Hotchkiss, S. (2009). Landscape-level variation in forest structure and biogeochemistry across a substrate age in Hawaii. *Ecology, 90*, 3074–3086.

Wright, S. J. (2005). Tropical forests in a changing environment. *Trends in Ecology & Evolution, 20*, 553–560.

Wright, S. J., & Van Schaik, C. P. (1994). Light and the phenology of tropical trees. *The American Naturalist, 143*, 192–199.

Zhang, J., Rivard, B., Sanchez-Azofeifa, A., & Castro-Essau, K. (2006). Intra- and inter-class spectral variability of tropical tree species at La Selva, Costa Rica: Implications for species identification using HYDICE imagery. *Remote Sensing of Environment, 105*, 129–141.


Please cite this article as: Somers, B., et al., Mesoscale assessment of changes in tropical tree species richness across a bioclimatic gradient in Panama using airborne imaging s..., *Remote Sensing of Environment* (2015), http://dx.doi.org/10.1016/j.rse.2015.04.016